Synthesis and Conformational Analysis of the T-Antigen Disaccharide (β-D-Gal-(1→3)-α-D-GalNAc-OMe)

Ralph Bukowski,[a] Laura M. Morris,[b] Robert J. Woods,[b] and Thomas Weimar*[a]

Dedicated to Prof. Joachim Thiem on the occasion of his 60th birthday.

Keywords: Carbohydrates / Conformation analysis / Molecular dynamics / NMR spectroscopy

We report an improved synthesis of the T-antigen disaccharide [β-D-Gal-(1→3)-α-D-GalNAc-OMe], incorporating recycling of the undesired β-glycosyl acceptor [methyl 2-azido-4,6-benzylidene-2-deoxy-β-D-galactopyranoside (**9β**)] through anomerization by treatment with $FeCl_3$. The conformational analysis of the disaccharide made use of high quality NOE data in combination with extensive Metropolis Monte-Carlo (MMC) and molecular dynamic (MD) simulations. To sample the conformational space sufficiently, $9.5 \cdot 10^6$ Monte-Carlo steps were collected for the MMC simulations, while the fully solvated MD simulations were performed for 10 ns for comparison. In general, the MMC and MD simulations agreed very well. Comparison of theoretical NOE curves from both MMC and MD simulations with the experimental curves showed that the disaccharide populates two regions of conformational space, with a population of about 95% for the global minimum energy region and about 5% for a local minimum energy region.

Introduction

The appearance in proteins of the disaccharide β-D-Gal-(1→3)-α-D-GalNAc (core 1), linked through the oxygen atom of a serine or threonine residue, can have varying biological significance, depending on the environment in which it occurs. When presented on the surface of erythrocytes it signals the end of the life cycle of the red blood cells, which are then disposed of in the liver. The disaccharide is also found in mucin-type glycoproteins[1] and in antifreeze glycoproteins in arctic fish.[2] In human tissues, outside the blood system, the presence of this disaccharide on cells is very often associated with carcinomas, and because of this it has been called the Thomson−Friedenreich antigen, or T-antigen.[3,4] Investigations of the mechanism of biological recognition of the T-antigen are, therefore, of wide interest, being particularly relevant for diagnostic or therapeutic purposes. In order to pursue mechanistic studies of this recognition process using nuclear magnetic resonance (NMR) spectroscopy, surface plasmon resonance, or microcalorimetry experiments, it was necessary to synthesize multi-milligram quantities of the disaccharide. We report here an improved synthesis of the target molecule [β-D-Gal-(1→3)-α-D-GalNAc-OMe (**13**)]. Additionally, we present a conformational analysis of the T-antigen disaccharide, based on high quality nuclear Overhauser enhancement (NOE) data combined with extensive computational simulations, which is a preliminary step in understanding the molecular recognition of the T-antigen disaccharide. Although the T-antigen structure has already been the focus of previous conformational analyses,[5−10] most of these were limited by relatively low quality experimental data. For the disaccharide in solution, typically only one interglycosidic NOE intensity (H1′−H3) was reported; this is insufficient to characterize the conformational properties of a glycosidic linkage uniquely.[6−8] In antifreeze glycoproteins, a NOE between H1′ and H4 has been observed, suggesting that, when linked to a protein backbone, the disaccharide adopts a different conformation than when free in solution.[5]

Results and Discussion

Synthesis

The synthesis of the T-antigen disaccharide was achieved by following the synthetic route described by Paulsen and co-workers,[11−14] with the incorporation of several improved protocols for the synthesis of intermediate products (Scheme 1 and 2). In particular, in the preparation of the donor molecule **3**, ammonium carbonate was used as a mild selective deprotection agent to obtain a free anomeric hydroxyl group in **2**,[15−17] which was then converted into the trichloroacetimidate **3**.[16,17] To avoid neighboring group effects, which would result in a β-glycosidic linkage adjacent to the *N*-acetyl group of the disaccharide, an azido function was introduced prior to formation of the methyl glycoside. Therefore, the galactosyl acceptor **9α** was prepared from galactal **5** by the azido-nitrate method[18] and subsequently benzylidenated to give an anomeric mixture of **9α** and **9β** (40% α, 60% β). At this stage, it was possible to separate the α and β products on silica gel. The direct transformation of

[a] Institut für Chemie, Medizinische Universität zu Lübeck, Ratzeburger Allee 160, 23538 Lübeck, Germany
Fax: (internat.) +49 451 500 4241
E-mail: thomas.weimar@chemie.mu-luebeck.de
[b] Complex Carbohydrate Research Center, 220 Riverbend Road, Athens, Georgia 30602−4712, USA

  1434−193X/01/0714−2697 $ 17.50+.50/0

the azido-nitrate mixture **6α/6β** into the methyl glycosides **7α/7β** considerably shortened the preparation of the glycosyl donor (**9α/9β**), in comparison to previously published approaches. The undesired anomer **9β** was subsequently deprotected, acetylated and anomerized by treatment with $FeCl_3$ in dichloromethane.[19] This produced an anomeric ratio of 85% α: 15% β for the azides **7α/7β**, which were then reintroduced into the synthetic route for the acceptor **9α**.

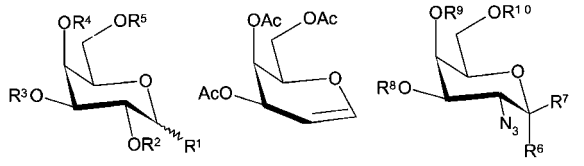

1-4 **5** **6-9**

	R^1	R^2	R^3	R^4	R^5
1	OAc	Ac	Ac	Ac	Ac
2	OH	Ac	Ac	Ac	Ac
3	$OC(NH)CCl_3$	Ac	Ac	Ac	Ac
4	Br	Ac	Ac	Ac	Ac

	R^6	R^7	R^8	R^9	R^{10}
6a	ONO_2	H	Ac	Ac	Ac
6b	H	ONO_2	Ac	Ac	Ac
7a	OMe	H	Ac	Ac	Ac
7b	H	OMe	Ac	Ac	Ac
8a	OMe	H	H	H	H
8b	H	OMe	H	H	H
9a	OMe	H	H	>CHPh	
9b	H	OMe	H	>CHPh	

Scheme 1. Synthesis scheme for the glycosyl donor and the acceptor molecules

The two protected monosaccharides (**3** and **9α**) were coupled to give **10** (Scheme 2). After deprotection of **10** and *O*-acetylation, the azido function was converted into an amide with thioacetic acid to give the T-antigen disaccharide **13** after *O*-deacetylation. Since most of the intermediate compounds prepared in this synthetic route were inadequately characterized by NMR in the literature, we report extensive ^1H and ^{13}C NMR spectroscopic data of these compounds in the materials and methods section.

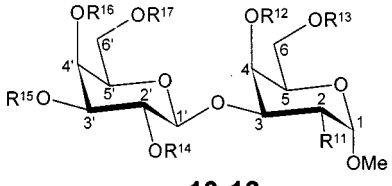

10-13

	R^{11}	R^{12}	R^{13}	R^{14}	R^{15}	R^{16}	R^{17}
10	N_3	>CHPh		Ac	Ac	Ac	Ac
11	N_3	Ac	Ac	Ac	Ac	Ac	Ac
12	NHAc	Ac	Ac	Ac	Ac	Ac	Ac
13	NHAc	H	H	H	H	H	H

Scheme 2. Synthesis scheme for the deprotection of the disaccharide. The numbering of the carbon atoms of the T-antigen disaccharide is indicated

NMR Spectroscopy of the T-Antigen Disaccharide

Full ^1H and ^{13}C assignments of T-antigen disaccharide **13** were achieved with conventional 1D and 2D NMR experiments (HMQC, COSY, TOCSY, NOESY). Homonuclear $^3J_{H,H}$ coupling constants were obtained from 1D ^1H experiments. All chemical shifts and $^3J_{H,H}$ coupling constants were in agreement with previously published data for the disaccharide or related compounds.[6−9] At 500 MHz, most of the proton resonances of **13** were well resolved (compare Figure 1); only the resonances of the two hydroxymethyl groups were degenerate. This allowed a complete set of NOE intensities to be acquired and integrated with the aid of 2D NOESY experiments in D_2O. Since NOE intensities for a disaccharide at 500 MHz and ambient temperature are usually very small, an experimental temperature of 316 K was chosen for the NOESY experiments. This placed the residual water signal between the resonances of H1 and H1′ and resulted in larger NOE intensities, due to the shortening of the correlation time for the molecule at higher temperature.

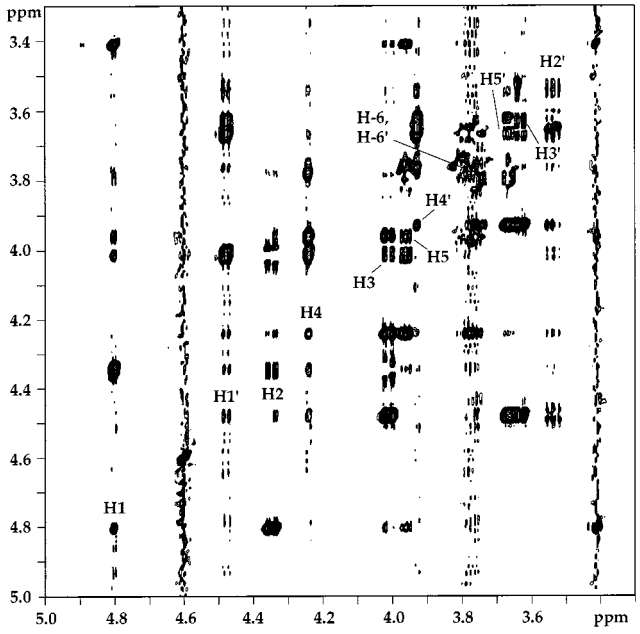

Figure 1. Section of a NOESY spectrum of **13** with 1.1 s mixing time

From a set of seven NOESY spectra, with mixing times between 100 ms and 1.3 s, it was possible to quantify both intraglycosidic and interglycosidic NOEs. The small intraglycosidic NOEs between H2 and H4 and between H2′ and H4′ (compare Figure 1) correspond to distances of 3.7−3.8 Å in the fixed $^4C_1$ chair geometries of the monosaccharide moieties. Since we were able to observe even smaller NOEs (compare Table 1), we concluded that our NOE data were of high quality. The interglycosidic NOEs (H1′−H3, H1′−H4, H1′−H2, H1′−N*H*Ac, H2′−H3, H2′−H4, and H5′−H4) convey information about the distribution of different conformational families at the glycosidic linkage. However, most of these NOEs showed a maximum en-

hancement of less than ≈0.3% (see Table 1). Only the NOE between H1′ and H3 was large, with a maximum enhancement of more than 4%. Although the other interglycosidic NOEs were very small, it was obvious that only a distribution of different conformational families at the 1→3 glycosidic linkage could account for the observed effects. When the disaccharide was bound to *Maclura pomifera* agglutinin, a trNOE between H1′ and H4, of approximately the same size as the H1′−H3 trNOE,[20] was observed. This observation implied that the 1→3 glycosidic linkage in **13** can adopt different conformational distributions when the carbohydrate interacts with a protein. For the free disaccharide, force field calculations (Figure 2) indicated that the molecule populates two main regions of conformational space.[10] To define the flexibility of the glycosidic linkage in **13** more accurately, we performed MMC and MD simulations and compared theoretical NOE intensities computed from these simulations with the experimental data.

Table 1. Compilation of interglycosidic and intraglycosidic NOE contacts of **13** in comparison to proton-proton distances derived from $A_{min,Gegop}$ and $B_{min,Gegop}$

	NOE [%]	Distance [Å]	
		$A_{min,Gegop}$	$B_{min,Gegop}$
H1−H2	4.55	2.43	2.43
H2−H4	0.38	3.78	3.78
H2′−H4′	0.44	3.85	3.85
H1′−H5′	4.44	2.28	2.28
H1′−H2	0.20	3.92	4.52
H1′−H3	4.79	2.39	3.51
H1′−H4	0.29	4.20	4.26
H1′−NHAc	0.12	3.84	5.53
H2′−H3	0.13	4.33	2.15
H2′−H4	0.12	4.43	2.39
H5′−H4	0.09	5.07	5.85

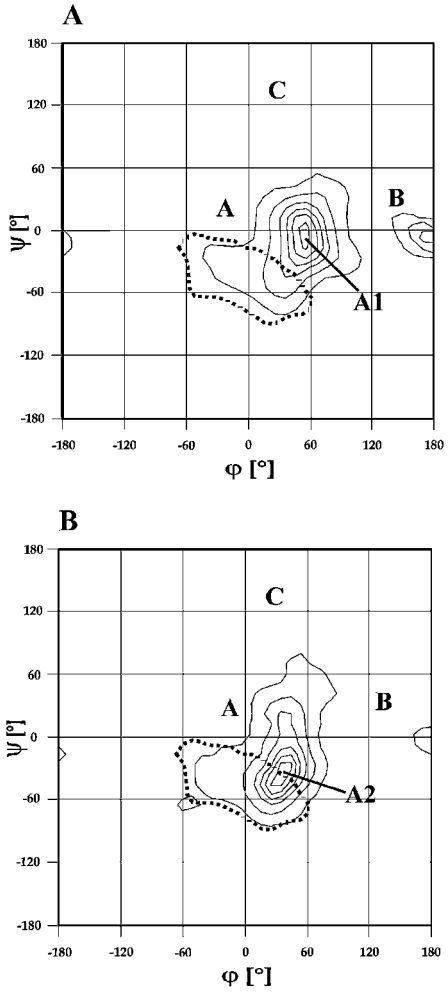

Figure 2. Population plot of the MMC ($3\cdot10^6$ MMC steps) and MD simulations of disaccharide **13**, showing the relative population of conformational space at the β-(1→3) linkage. The contours were calculated by dividing the φ/ψ population maps from MMC and MD simulations into bins of 10° spacing in both directions. The number of conformations in every bin was counted, and contour levels were then calculated relative to the highest populated bin. The contour levels define regions with (from the inside to the outside of the contour plot) >90%, 70−90%, 50−70%, 30−50%, 10−30%, and 1−10% of the number of conformations in the highest populated bin. The dotted lines encircle the regions of conformational space in which the distance between protons H1′ and H4 is shorter than 3 Å. Conformations A1, A2, and B are displayed in Figure 3

MMC Simulations

A total of $9.5\cdot10^6$ Monte-Carlo steps were collected for the MMC simulations. A temperature factor of 600 K, which had previously been found to reproduce experimental data very well,[21] was used in the calculations. The population map (Figure 2, A) was created from a simulation of this type, and shows two regions of conformational space (A and B) in which the majority of conformations of **13** were located. The results from the simulations were independent of the starting conformation, which indicated that the conformational space had been sampled long enough to reach equilibrium. Even when a starting conformation far outside region A or B was chosen, the simulation converged rapidly to the preferred conformational space shown in Figure 2, A. In the resulting population map, ≈95% of conformations are found in region A and ≈5% in region B. When MMC simulations were performed with a temperature factor of 2000 K, a third region of conformational space (C, φ/ψ ≈ 30°/155°) was also found to be populated (compare below). On the basis of the population map, the minimum energy conformations $A_{min,Gegop}$ and $B_{min,Gegop}$ of **13** were found at the glycosidic angles φ/ψ = 52.5°/7.9° (relative potential energy $E_{pot,Gegop}$ = 0.0 kcal mol^{-1}) and φ/ψ = 170.6°/−2.0° (relative potential energy $E_{pot,Gegop}$= 1.1 kcal mol^{-1}), respectively. In minimum energy conformation $B_{min,Gegop}$, short distances were found between the proton pairs H2′−H3 and H2′−H4 (compare Table 1 and Figure 3). Since the corresponding NOEs for these interactions were very weak (≈0.1%), the experimental data are consistent with a minimal (but finite) population of the B conformation in solution, corresponding very well with the results of the MMC and the MD (see below) simulations.

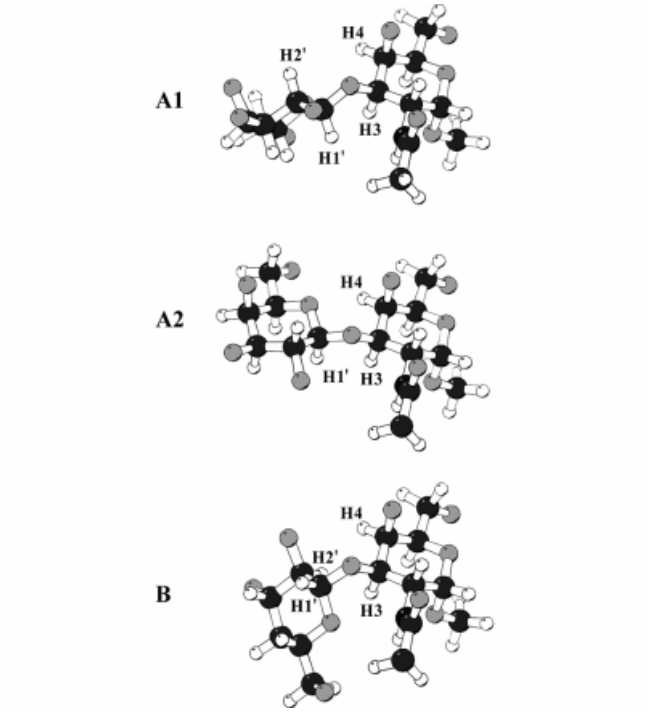

Figure 3. Ball and stick representations of conformations A1 and B from MMC and A2 from MD simulations of **13** (produced with Molscript[32]). Hydroxyl protons have been omitted for clarity. Nitrogen atoms are black, carbon atoms dark gray, and oxygen atoms light gray

MD Simulations

In order to determine the dependence of the simulation on the starting conformation, we initiated five simulations from stable conformations previously identified by adiabatic energy mapping.[10] Each simulation was allowed to continue for 1000 ps. After that time, all simulations had converged to essentially equivalent distributions (data not shown), with the exception of the simulation initiated from conformation C. No transitions out of conformation C were observed at 300 K, suggesting that significantly high energy barriers exist around this structure. This conclusion is further supported by the observation that no transitions into conformation C were observed to occur from any of the simulations initiated from the alternate conformations, even after extension of the simulation to 10 ns (see Figure 2, B). Because of the absence of transitions into or out of conformation C, it is not possible to determine whether it is higher or lower in energy than the other conformations. However, the fact that it was only observed in the MMC simulations when a higher temperature factor was employed is consistent with this conformation being higher in energy.

The molecular dynamics simulations are considerably longer than those typically performed and allowed us to compare the statistical distribution of conformers at 300 K in solvated simulations with that predicted from adiabatic energy mapping and Monte-Carlo simulations. The majority of the structures fell into the A region, which displays φ

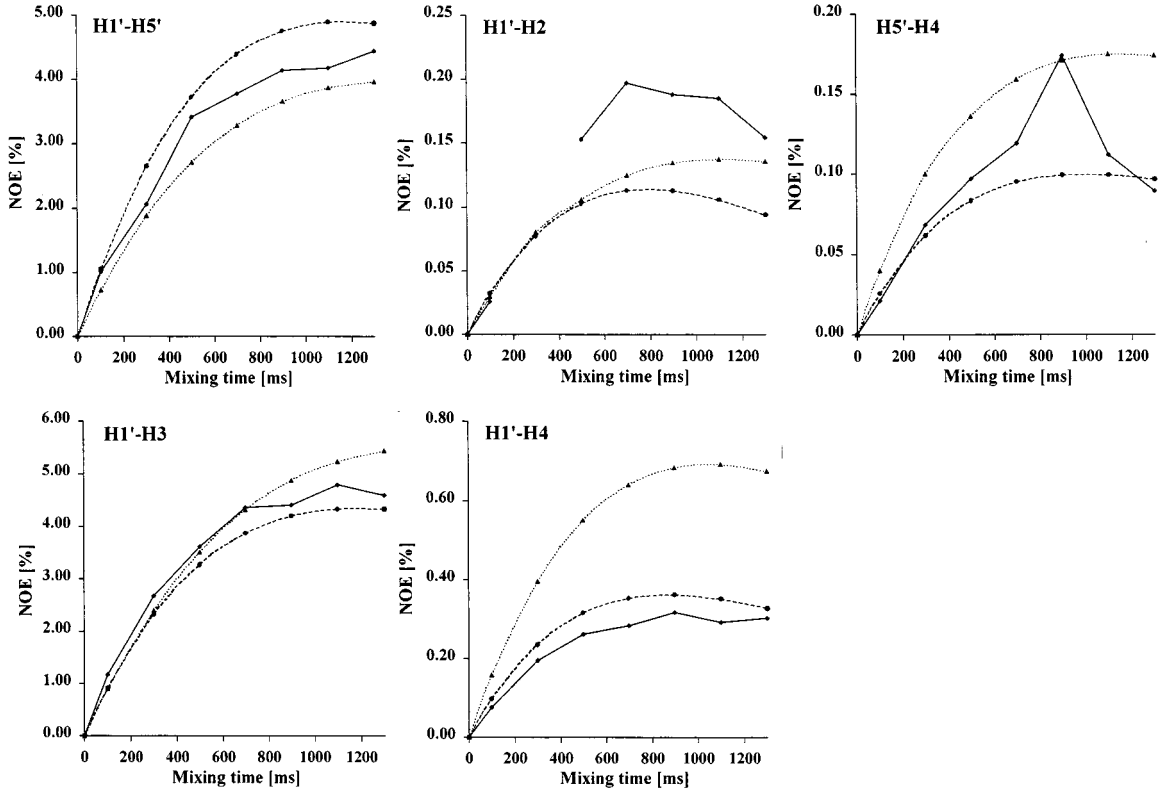

Figure 4. Selected interglycosidic NOE curves of **13**. Experimental data solid lines, MD data dotted, and MMC data dashed. For the NOE between H1′ and H2 the experimental data point at 300 ms mixing time is missing

angles consistent with the *exo*-anomeric effect (≈ +60°, see Figure 2, B, and Figure 3); other conformations are only minimally populated. The simulations further indicated that the presence of conformation C was not required for agreement with experiment (see below).

Comparing Experimental NOEs with Theoretical NOEs

Theoretical NOE curve-fitting of the MMC data was best achieved with an overall correlation time (τ_c) of 70 ps. We therefore used this correlation time to calculate theoretical NOE data from the MMC and the MD simulations. As can be seen from the NOE curves in Figure 4, most of the theoretical NOE data correspond very well with the experimental curves. This is an important achievement, given the small size of the inter-glycosidic NOEs between H1′ and H2 and between H5′ and H4. For the small interglycosidic NOE between H1′ and H4, the MMC simulations gave a better fit to the experimental data than the MD simulations do. This reflects the fact that the distribution of conformational families differs between the MMC and MD simulations. In the region of conformational space in which short distances between the corresponding protons are found, the MD simulations show a larger number of conformations than the MMC simulations do (compare Figure 2). Simple model building showed that, in conformation C, a short distance exists between the oxygen atom of the hydroxymethyl group of the galactosyl residue and the *N*-acetyl group of the galactosaminyl residue (≈ 2.1 Å). A hydrogen bond between OH6 of the galactosyl residue and the carbonyl oxygen of the galactosamine might enhance the stability of this conformation. However, the origin of the high barrier to the formation of conformation C remains unclear. No NOEs indicative of conformation C were observed in solution, which is consistent with the simulations. In summary, both simulations had succeeded in adequately sampling the conformational space of **13**.

Conclusion

We have improved the synthetic route to the T-antigen disaccharide **13** by incorporating some modern protocols for the synthesis of intermediate products. Recycling of the unwanted benzylidene derivative **9β** resulted in a significantly increased overall yield of the desired product. The synthesis constitutes the basis for extensive interaction studies of the T-antigen with lectins that bind this carbohydrate specifically, such as *Jacalin* and *Maclura pomifera* agglutinin.

The conformational analysis of the disaccharide took advantage of high quality NMR spectroscopic data, which provided the basis for a comparison of experimental NOEs with theoretical NOE data from MMC and MD simulations. These simulations were run considerably longer than usual, to ensure that the conformational space was sampled sufficiently. The results of the MD and the MMC simulations differed only slightly. Interestingly, both the MMC and MD simulations indicate that the φ-angle of the 1→3 glycosidic linkage populates not only the conformation consistent with the *exo*-anomeric effect (≈60°), but also a relatively uncommon one (≈180°). Comparison of the theoretical NOE data with experimental NOE data showed that the local minimum energy region B is populated in aqueous solution, but only to a small degree of ≈ 5%. This is the first time that this local minimum energy region has been detected experimentally, and its presence suggests that the T-antigen disaccharide is more flexible than thought previously. This *anti*-φ conformational family was recently also found to be populated in β-(1→2) linkages[22] and in glycomimetics.[23,24]

The conformational analysis forms the basis for the interpretation of lectin-bound conformations of the disaccharide. A first result of the recognition of the T-antigen by *Maclura pomifera* agglutinin is that the conformation at the β-(1→3) glycosidic linkage of the disaccharide in solution is different[20] from that in the previously published crystal structure.[25]

Experimental Section

Abbreviations: MD, molecular dynamics; MMC, Metropolis Monte-Carlo; $A_{min,Gegop}$, $B_{min,Gegop}$, minimum energy conformations (A and B) found with Gegop; $E_{pot,Gegop}$, potential energy of the minimum energy conformation found with Gegop; TSP, (3-trimethylsilyl)propionic acid; ea, ethyl acetate; hx, hexane.

Additional material available: The GLYCAM parameters are freely available from Dr. Woods (http://glycam.ccrc.uga.edu). The Gegop program can be obtained at http://sgi1.chemie.uni-hamburg.de.

NMR Spectroscopy: All NMR experiments were performed on a Bruker DRX 500 spectrometer. Spectra recorded in $CDCl_3$ are referenced to the residual $CHCl_3$ signal at δ = 7.30 (^{1}H) or δ = 77.00 (^{13}C), spectra recorded in D_2O are referenced to TSP. NMR spectroscopic data for **13** were acquired at 316 K. The sample contained 6 mg (MW 397, 15.1 mmol) of the disaccharide in D_2O. Exchangeable protons were removed by repeatedly dissolving and lyophilizing the sample from D_2O. 2D NOESY spectra were recorded with eight scans, 4 K data points (t2) and 512 increments (t1) at mixing times of 100, 300, 500, 700, 900, 1100, and 1300 ms. Prior to Fourier transformation, which used a squared cosine function for apodization, the data were zero-filled to give a final data matrix of 8K × 1K (F2 × F1). After the Fourier transformation, the spectra were base plane corrected. The processed spectra were integrated with AURELIA (Bruker). All NOE intensities are scaled to the diagonal signal of H4, which was extrapolated to 100% at zero mixing time.

Computations

Glycosidic torsional angles are defined using the protons, as φ(H1′−C1′−O1′−C*x*), ψ(C1′−O1′−C*x*−H*x*) and ω(O6−C6−C5−O5), with *x* being the aglyconic site.

MMC Calculations: MMC simulations were performed on Silicon Graphics O2 workstations with Gegop (*Geometry of Glycoproteins)* 2.7.[26] The simulations used temperature parameters of 600 K and 2000 K and up to $9.5 \cdot 10^6$ Monte-Carlo steps. The maximum allowed step length for the dihedral angles was 35° for the angles of the β-(1→3) linkage and 75° for the ω angles, which led to acceptances rates in the range of 35−40%. Energy minimizations were

performed using the Davidon−Fletcher−Powell algorithm. Theoretical NOEs were calculated using the full relaxation matrix approach[27,28] [$(r^{-3})^2$ averaging], which is build into Gegop for correlation times (τ_c) in the range between 5 and 150 ps.

MD Simulations: The simulations were performed under constant pressure (1 atm.) and temperature (300 K) conditions with the AMBER 5.0 force field, employing the GLYCAM parameters for simulations of oligosaccharides and glycoproteins[29] on a Silicon Graphics Octane computer. The carbohydrate was solvated in a box of 623 TIP3P water molecules of approximate dimensions (31 × 29 × 26 Å). Initial conformations were selected from adiabatic energy maps[10]. The initial configurations were energy-minimized in solvent using a steepest descent protocol for 3000 minimization cycles. The simulations were initiated by assigning random atomic velocities from a Boltzmann distribution at 5 K. The temperature of the system was then raised to 300 K over a period of 50 ps, with separate temperature couplings for the solute (0.25 ps^{-1}) and solvent (0.25 ps^{-1}). As recommended for simulations employing recent versions of the AMBER force field,[30] 1-4-nonbonded electrostatic interactions were scaled by a standard factor of 1:1.2. A residue-based cut-off for nonbonded interactions of 8 Å was selected and is consistent with the TIP3P water model. The principal simulation, when initiated from conformation A1,[10] was maintained at 300 K for 10 ns. Other simulations were run for shorter times (1000 ps) as discussed in the text. The CORMA program[31] was used to compute NOE intensities from a full relaxation matrix analysis of 2500 frames taken from the 10 ns MD trajectory (frames saved at 4 ps intervals).

Syntheses

General Methods: Merck 60 F_{254} silica gel plates were used for TLC. Compounds were viewed by treatment with a solution of sulfuric acid in ethanol and subsequent heating. Melting points were measured with a Büchi 510 apparatus. − Optical rotations were determined with a Perkin−Elmer 243B polarimeter for solutions in chloroform and water. − For the activation of zinc, zinc dust (39.02 g, 0.597 mmol) was stirred with 10% HCl, filtered, washed with water, acetone, and diethyl ether, and dried in vacuo before use.

1,2,3,4,6-Penta-*O*-acetyl-D-galactopyranoside (1):[33] A mixture of D-galactose (10.02 g, 55.7 mmol), acetic anhydride (60 mL), and pyridine (65 mL) was stirred at room temperature overnight. After 20 h, remaining acetic anhydride was hydrolyzed with water. The aqueous solution was extracted three times with chloroform, and the combined organic phases were washed with satd. sodium hydrogen carbonate solution and dried with sodium sulfate. After filtration and removal of residual pyridine by azeotropic distillation with toluene, a pale yellow substance (20.4 g, 94.3%) was isolated and used without further purification for the synthesis of **2** and **4**; R_f = 0.6 in ea/hx 2:1, 0.46 in ea/hx 1:1.

2,3,4,6-Tetra-*O*-acetyl-D-galactopyranose (2):[15] A solution of **1** (20.3 g, 52.2 mmol) in dry dimethylformamide (100 mL) was stirred at 30 °C with ammonium carbonate (10.0 g, 0.104 mol). After 22 h, chloroform (100 mL) was added and the mixture was poured into hydrochloric acid (1 M, 300 mL), with ice cooling. The aqueous phase was washed three times with chloroform (100 mL), and the combined organic phases were neutralized with satd. sodium hydrogen carbonate solution and dried with sodium sulfate. After filtration, removal of the solvent in vacuo, and azeotropic distillation with butanol/water, toluene, and dichloromethane, an orange oil remained. Filtration over silica gel with hx/ea 1:10, removal of the solvent, and azeotropic distillation with toluene and dichloromethane yielded a colorless foam (11.4 g, 62.8%), which was used without further purification for the synthesis of **3**; R_f = 0.21 in ea/hx 2:1, 0.58 in ea/hx 10:1.

***O*-(2,3,4,6-Tetra-*O*-acetyl-α-D-galactopyranosyl)trichloroacetimidate (3):**[16,17] A solution of **2** (3.0 g, 8.62 mmol) in dichloromethane (25 mL) was stirred with trichloroacetonitrile (1.5 mL, 15.0 mmol) and cesium carbonate (201 mg, 1.04 mmol) at room temperature for 30 h. The mixture was washed with 50 mL of water and satd. sodium chloride solution. The organic phase was dried with sodium sulfate and treated with active carbon. After filtration and removal of the solvent, a pale yellow oil was isolated and subjected to column chromatography (*l*: 38 cm, *d*: 3.5 cm, chloroform). The solvent was removed under reduced pressure. A colorless, crystalline substance was isolated (3.56 g, 83.9%); m.p. 103−106 °C; R_f = 0.57 in ea/hx 2:1. − ^{1}H NMR ($CDCl_3$): δ = 2.03, 2.04, 2.05, 2.19 (s, 12 H, 4 CH_3CO), 4.07−4.24 (m, 2 H, $J_{5,6ab}$ = 6.59 Hz, $J_{6a,6b}$ = 11.25 Hz, H6a, H6b), 4.49 (dt, 1 H, $J_{4,5}$ = 1.23 Hz, H5), 5.15 (dd, 1 H, $J_{1,2}$ = 3.57, $J_{2,3}$ = 10.57 Hz, H2), 5.38 (dd, 1 H, $J_{3,4}$ = 3.57 Hz, H3), 5.48 (dd, 1 H, H4), 6.62 (d, 1 H, H1), 8.70 (s, 1 H, NH). − ^{13}C NMR ($CDCl_3$): δ = 20.5, 20.53, 20.57, 20.59 (s, 4 C, 4 *C*H_3CO), 61.2, 66.8, 67.3, 67.4, 68.9, 93.5 (s, 6 C, C1, C2, C3, C4, C5, C6), 160.9 (s, 1 C, NH*C*CCl_3), 169.9, 170.02, 170.05, 170.2 (s, 4 C, 4 CH_3*C*O).

2,3,4,6-Tetra-*O*-acetyl-α-D-galactopyranosyl Bromide (4):[33,34] An ice-cooled 33% solution of hydrobromic acid (115 mL, 0.61 mmol) was added dropwise to a solution of **1** (22.3 g, 57.2 mmol) in glacial acetic acid (100 mL) and stirred overnight, during which time the mixture was allowed to warm to room temperature. The solution was poured into a mixture of ice and water and the aqueous solution was extracted several times with chloroform. The combined organic phases were washed with satd. sodium hydrogen carbonate solution and water. After drying with sodium sulfate and filtration, the solvent was evaporated in vacuo. A pale yellow syrup remained (21.7 g, 92.3%); R_f = 0.57 in ea/hx 2:1. − ^{1}H NMR ($CDCl_3$): δ = 2.01, 2.06, 2.12, 2.15 (s, 12 H, 4 CH_3CO), 4.09−4.21 (m, 2 H, $J_{5,6ab}$ = 6.59 Hz, $J_{6a,6b}$ = 11.39 Hz, H6a, H6b), 4.49 (ddd, 1 H, $J_{4,5}$ = 1.23 Hz, H5), 5.05 (dd, 1 H, $J_{1,2}$ = 3.98, $J_{2,3}$ = 10.57 Hz, H2), 5.41 (dd, 1 H, $J_{3,4}$ = 3.29 Hz, H3), 5.52 (dd, 1 H, H4), 6.70 (d, 1 H, H1). − ^{13}C NMR ($CDCl_3$): δ = 20.2, 20.3, 20.4, 20.7 (s, 4 C, 4 *C*H_3CO), 60.6, 66.7, 67.5, 67.7, 70.8, 88.1 (s, 6 C, C1, C2, C3, C4, C5, C6), 169.4, 169.6, 169.7, 170.0 (s, 4 C, 4 CH_3*C*O).

3,4,6-Tri-*O*-acetyl-D-galactal (5):[34,35] A suspension of activated zinc dust (21.9 g, 0.335 mol) in ethyl acetate (225 mL) and *N*-methylimidazole (4.5 mL) was refluxed and a solution of **4** (22.9 g, 55.7 mmol) in dry ethyl acetate (70 mL) was added dropwise. The mixture was subsequently heated for another hour, then filtered through Celite®, washed with 10% hydrochloric acid and satd. sodium hydrogen carbonate solution, and dried with sodium sulfate. After filtration, the solvent was evaporated in vacuo. The residual yellow oil was subjected to column chromatography (*l:* 19 cm, *d:* 5 cm, ea/hx 2:1). Removal of the solvent under reduced pressure and azeotropic distillation with toluene and dichloromethane yielded a colorless syrup (11.9 g, 78.7%); R_f = 0.58 in ea/hx 2:1. − ^{1}H NMR ($CDCl_3$): δ = 2.03, 2.09, 2.13 (s, 9 H, 3 CH_3CO), 4.19−4.32 (m, 2 H, $J_{5,6a,b}$ = 5.21 Hz, $J_{6a,6b}$ = 11.39 Hz, H6a, H6b), 4.33 (m, 1 H, $J_{4,5}$ = 1.78 Hz, H5), 4.74 (ddd, 1 H, $J_{1,2}$ = 6.31, $J_{2,3}$ = 1.37 Hz, H2), 5.43 (dt, 1 H, $J_{3,4}$ = 4.53 Hz, H4), 5.56 (m, 1 H, $J_{1,3}$ = 1.78 Hz, H3), 6.47 (dd, 1 H, H1). − ^{13}C NMR ($CDCl_3$): δ = 20.6, 20.72, 20.78 (s, 3 C, 3 *C*H_3CO), 61.9, 63.7, 63.9, 72.8 (s, 4 C, C3, C4, C5, C6), 98.8 (s, 1 C, C2), 145.4 (s, 1 C, C1), 170.1, 170.52, 170.53 (s, 3 C, 3 CH_3*C*O).

3,4,6-Tri-*O*-acetyl-2-azido-2-deoxy-α/β-D-galactopyranosyl Nitrate (6α/6β):[18] A solution of **5** (3.8 g, 13.97 mmol) in dry acetonitrile (80 mL) was added with cooling (−15 to −20 °C) over 45 min to a mixture of sodium azide (1.39 g, 21.4 mmol) and ceric(IV) ammonium nitrate (22.85 g, 41.7 mmol). After six hours, ice-cold diethyl ether and ice water were added, and the organic layer was separated, washed several times with ice water until it was colorless, and dried with sodium sulfate. The organic layer was then filtered and the solvent evaporated in vacuo. Further purification of the orange oil was performed by a column chromatography (*l:* 16 cm, *d:* 5 cm, ea/hx 1:1). A pale yellow syrup was isolated after removal of the solvent and azeotropic distillation with toluene and dichloromethane. This syrup consisted of the two anomers **6α** and **6β** (2.68 g, 51.0%). α anomer: m.p. 101−103 °C, ref. 103−104 °C; R_f = 0.64 in ea/hx 1:1; β anomer: m.p. 127−130 °C; R_f = 0.38 in ea/hx 1:1. − ^{1}H NMR (α anomer **6α**, $CDCl_3$): δ = 2.04, 2.08, 2.17 (s, 9 H, 3 CH_3CO), 4.09−4.15 (m, 2 H, H6a, H6b), 4.05 (m, 1 H, $J_{4,5}$ = 1.10 Hz, H5), 4.12 (dd, 1 H, $J_{1,2}$ = 4.12, $J_{2,3}$ = 11.25 Hz, H2), 5.25 (dd, 1 H, $J_{3,4}$ = 3.16 Hz, H3), 5.50 (dd, 1 H, H4), 6.34 (d, 1 H, H1). − ^{13}C NMR (α anomer **6α**, $CDCl_3$): δ = 20.53, 20.57, 20.6 (s, 3 C, 3 *C*H_3CO), 55.8, 61.0, 65.8, 68.6, 69.5 (s, 5 C, C2, C3, C4, C5, C6), 92.0 (s, 1 C, C1), 170.04, 170.06, 170.3 (s, 3 C, 3 CH_3*C*O). − ^{1}H NMR (β anomer **6β**, $CDCl_3$): δ = 2.00, 2.05, 2.13 (s, 9 H, 3 CH_3CO), 3.83 (dd, 1 H, $J_{1,2}$ = 8.9, $J_{2,3}$ = 10.6 Hz, H2), 4.07 (dt, 1 H, $J_{4,5}$ = 0.82 Hz, $J_{5,6ab}$ = 6.59 Hz, H5), 4.11−4.19 (m, 2 H, $J_{6a,6b}$ = 11.39 Hz, H6a, H6b), 5.10 (dd, 1 H, $J_{3,4}$ = 3.43 Hz, H3), 5.43 (dd, 1 H, H4), 5.71 (d, 1 H, H1). − ^{13}C NMR (β anomer **6β**, $CDCl_3$): δ = 20.4, 20.5, 20.7 (s, 3 C, 3 *C*H_3CO), 57.5, 66.7, 67.7, 70.7, 71.6 (s, 5 C, C2, C3, C4, C5, C6), 96.8 (s, 1 C, C1), 168.9, 169.2, 169.3 (s, 3 C, 3 CH_3*C*O).

Methyl 3,4,6-Tri-*O*-acetyl-2-azido-2-deoxy-α/β-D-galactopyranoside (7α/7β):[13] The anomeric mixture **6α/6β** (2.68 g, 7.13 mmol) was dissolved in dry methanol (12 mL) and stirred with a solution of sodium (200 mg, 8.7 mmol) in dry methanol (6 mL), with ice-cooling, for 30 min. The solution was neutralized with Amberlite® IR-120, mixed with active carbon, filtered, and evaporated in vacuo. The product was acetylated overnight with acetic anhydride and pyridine. The solution was evaporated in vacuo and co-distilled with toluene and dichloromethane. The residue was dissolved in a mixture of ea/hx 1:1, mixed with active carbon, and filtered through a layer of sodium sulfate, silica gel, and sodium sulfate, evaporated in vacuo, and co-distilled with toluene and dichloromethane. A yellow oil composed of the α and β anomers was isolated (2.27 g, 92.3%); R_f = 0.52 in ea/hx 1:1, 0.65 in ea/hx 2:1. − ^{1}H NMR (**7α**, $CDCl_3$): δ = 2.08, 2.18, 2.20 (s, 9 H, 3 CH_3CO), 3.49 (s, 3 H, OCH_3), 3.72 (dd, 1 H, $J_{1,2}$ = 3.30, $J_{2,3}$ = 11.00 Hz, H2), 4.11−4.25 (m, 3 H, H5, H6a, H6b), 4.93 (d, 1 H, H1), 5.38 (dd, 1 H, $J_{3,4}$ = 3.30 Hz, H3), 5.48 (dd, 1 H, $J_{4,5}$ = 0.92 Hz, H4). − ^{13}C NMR (**7α**, $CDCl_3$): δ = 20.4−20.6 (m, 3 C, 3 *C*H_3CO), 55.5 (s, 1 C, OCH_3), 57.5, 66.3, 66.4, 67.5, 68.3 (s, 5 C, C2, C3, C4, C5, C6), 98.8 (s, 1 C, C1), 169.6, 169.9, 170.3 (s, 3 C, 3 CH_3*C*O). − ^{1}H NMR (**7β**, $CDCl_3$): δ = 2.08, 2.09, 2.19 (s, 9 H, 3 CH_3CO), 3.64 (s, 3 H, OCH_3), 3.69 (dd, 1 H, $J_{1,2}$ = 8.07, $J_{2,3}$ = 10.82 Hz, H2), 3.89 (dt, 1 H, $J_{4,5}$ = 0.92 Hz, $J_{5,6a}$ = 6.42 Hz, $J_{5,6b}$ = 7.15 Hz, H5), 4.15 (dd, 1 H, $J_{6a,6b}$ = 11.37 Hz, H6b), 4.22 (dd, 1 H, H6a), 4.31 (d, 1 H, H1), 4.83 (dd, 1 H, $J_{3,4}$ = 3.30 Hz, H3), 5.37 (dd, 1 H, H4). − ^{13}C NMR (**7β**, $CDCl_3$): δ = 20.4−20.6 (m, 3 C, 3 *C*H_3CO), 57.3 (s, 1 C, OCH_3), 60.7, 61.1, 61.6, 70.5, 71.0 (s, 5 C, C2, C3, C4, C5, C6), 103.0 (s, 1 C, C1), 169.7, 170.0, 170.2 (s, 3 C, 3 CH_3*C*O).

Methyl 3,4,6-Tri-*O*-acetyl-2-azido-2-deoxy-α-D-galactopyranoside (7α):[19] The anomeric mixture **7α/7β** (1.25 g, 3.62 mmol) was dissolved in dry dichloromethane (30 mL) and mixed with dry iron(III) chloride (780 mg, 4.81 mmol). The mixture was first stirred at room temperature for 4 days, then refluxed for 4.5 days. After addition of water, it was extracted several times with dichloromethane. The combined organic layers were dried with sodium sulfate, filtered, and evaporated in vacuo. The residue was stirred overnight with acetic anhydride and pyridine. After evaporation in vacuo and co-distillation with toluene, the residual substance was filtered through a layer of sodium sulfate, silica gel, and sodium sulfate (ea/hx 2:1), evaporated in vacuo, and co-distilled with toluene and dichloromethane. A yellow oil composed of 85% α and 15% β anomer was isolated (0.84 g, 67.2%).

Methyl 2-Azido-2-deoxy-α/β-D-galactopyranoside (8α/8β):[13] The anomeric mixture **7α/7β** (860 mg, 2.49 mmol) was dissolved in dry methanol (10 mL), stirred with a catalytic amount of a fresh solution of sodium in dry methanol for 30 min, neutralized with Amberlite® IR-120, filtered, and evaporated in vacuo. After column chromatography (*l:* 15 cm, *d:* 2.5 cm, $CHCl_3$/MeOH 5:4), evaporation, and azeotropic distillation with toluene and dichloromethane, a colorless solid was isolated (522.96 mg, 95.9%); m.p. >160 °C (decomp.); R_f = 0.63 in $CHCl_3$/MeOH 5:4. − ^{1}H NMR ($CDCl_3$): δ = 2.04, 2.14 (s, 9 H, 3 α-CH_3CO), 2.05, 2.15 (s, 9 H, 3 β-CH_3CO), 3.42 (s, 3 H, α-OCH_3), 3.49 (dd, 1 H, $J_{1,2}$ = 8.24, $J_{2,3}$ = 10.38 Hz, β-H2), 3.61 (s, 3 H, β-OCH_3), 3.67 (dd, 1 H, $J_{3,4}$ = 3.66 Hz, β-H3), 3.74 (dd, 1 H, $J_{1,2}$ = 8.24, $J_{1,2}$ = 3.66, $J_{2,3}$ = 10.68 Hz, α-H2), 3.69−3.83 (m, 4 H, α-H6a, α-H6b, β-H6a, β-H6b), 3.91 (d, 1 H, β-H4), 3.87−3.93 (m, 2 H, α-H5, β-H5), 3.95 (dd, 1 H, $J_{3,4}$ = 3.05 Hz, α-H3), 3.99 (d, 1 H, α-H4), 4.38 (d, 1 H, β-H1), 4.96 (d, 1 H, α-H1). − ^{13}C NMR ($CDCl_3$): δ = 54.9 (s, 1 C, α-OCH_3), 57.1 (s, 1 C, β-OCH_3), 60.9, 63.3, 68.0, 71.7, 75.2 (s, 5 C, β-C2, β-C3, β-C4, β-C5, β-C6), 60.3, 61.2, 68.5, 68.8, 70.9 (s, 5 C, α-C2, α-C3, α-C4, α-C5, α-C6), 98.1 (s, 1 C, α-C1), 102.6 (s, 1 C, β-C1).

Methyl 2-Azido-4,6-benzylidene-2-deoxy-α/β-D-galactopyranoside (9α/9β):[36] The anomeric mixture **7α/7β** (1.01 g, 2.93 mmol) was dissolved in dry methanol (10 mL), stirred with a catalytic amount of a fresh solution of sodium in dry methanol for 30 min, neutralized with Amberlite® IR-120, filtered, and evaporated in vacuo. The residue was stirred with benzaldehyde (5.0 mL, 49.2 mmol) and zinc chloride (548 mg, 4.02 mmol) at room temperature. After 4.5 days, chloroform was added, and the organic layer was extracted several times with a 39% solution of sodium hydrogen sulfite. The combined organic phases were dried with sodium sulfate, filtered, and evaporated in vacuo. The residual orange oil was chromatographed on silica gel (*l:* 27 cm, *d:* 2 cm, ea/hx 2:1). Both anomers were isolated separately as colorless syrups (**9α**: 456 mg [50.7%], **9β**: 218 mg [24.3%]); R_f (**9α**) 0.48 in ea/hx 2:1. − ^{1}H NMR (**9α**, $CDCl_3$): δ = 3.49 (s, 3 H, OCH_3), 3.68 (dd, 1 H, $J_{1,2}$ = 3.43, $J_{2,3}$ = 10.43 Hz, H2), 3.78 (m, 1 H, $J_{4,5}$ = 0.96 Hz, $J_{5,6a}$ = 1.92 Hz, $J_{5,6b}$ 1.65 Hz, H5), 4.14 (dd, 1 H, H6a), 4.21 (dd, 1 H, $J_{3,4}$ = 3.70 Hz, H3), 4.33 (dd, 1 H, H4), 4.34 (dd, 1 H, $J_{6a,6b}$ = 12.76 Hz, H6b), 4.95 (d, 1 H, H1), 5.63 (s, 1 H, PhC*H*), 7.37−7.41 (m, 3 H, *o*-/*p*-Ph), 7.68−7.73 (m, 2 H, *m*-Ph). − ^{13}C NMR ($CDCl_3$): δ = 55.7 (s, 1 C, OCH_3), 60.9, 62.6, 67.8, 69.2, 75.6, 99.6, 101.3 (s, 7 C, Ph*C*H, C1, C2, C3, C4, C5, C6), 126.2, 128.3, 128.5, 129.4, 130.2, 133.7 (s, 6 C, Ph).

Methyl *O*-(2,3,4,6-Tetra-*O*-acetyl-β-D-galactopyranosyl)-(1→3)-2-azido-4,6-benzylidene-2-deoxy-α-D-galactopyranoside (10): A solution of **9α** (214.0 mg, 0.697 mmol) and **3** (442.0 mg, 0.898 mmol) in dry 1,2-dichlorethane (20 mL) was stirred with molecular sieves (4 Å) under an atmosphere of dry N_2 at room temperature for 90 min. The solution was cooled to −18 °C and a solution of trimethylsilyl triflate (13.1 μL, 0.065 mmol) in 1,2-dichlorethane (3 mL) was added dropwise. After 15 min, the cooling was removed, and

the solution was diluted with dry 1,2-dichlorethane, neutralized with triethylamine, evaporated in vacuo, and chromatographed on silica gel (*l:* 27 cm, *d:* 3.5 cm, ea/hx 2:1). After removal of the solvent and azeotropic distillation with toluene and dichloromethane, a colorless solid was isolated (294.6 mg, 66.2%); m.p. 186−188 °C; $[\alpha]_D^{23}$ = +101.9 (*c* = 0.98, $CHCl_3$); R_f = 0.54 in ea/hx 2:1. − ^{1}H NMR ($CDCl_3$): δ = 1.98, 2.05, 2.06, 2.17 (s, 12 H, 4 CH_3CO), 3.67 (s, 1 H, H5), 3.91 (dd, 1 H, $J_{1,2}$ = 3.43, $J_{2,3}$ = 10.84 Hz, H2), 3.93 (dd, 1 H, $J_{4',5'}$ = 0.96 Hz, H5′), 4.07 (dd, 1 H, $J_{5,6a}$ = 1.51 Hz, H6a), 4.09 (dd, 1 H, $J_{3,4}$ = 3.16 Hz, H3), 4.12 (dd, 1 H, H6a′), 4.20 (dd, 1 H, $J_{5',6b'}$ = 6.59 Hz, $J_{6a',6b'}$ = 11.25 Hz, H6b′), 4.28 (dd, 1 H, $J_{5,6b}$ = 1.51 Hz, $J_{6a,6b}$ = 12.49 Hz, H6b), 4.37 (d, 1 H, H4), 4.78 (d, 1 H, $J_{1',2'}$ = 7.96 Hz, H1′), 4.93 (d, 1 H, H1), 5.02 (dd, 1 H, $J_{2',3'}$ = 10.43 Hz, $J_{3',4'}$ = 3.43 Hz, H3′), 5.29 (dd, 1 H, H2′), 5.40 (dd, 1 H, H4′), 5.65 (s, 1 H, PhC*H*), 7.33−7.41 (m, 3 H, *o*-/*p*-Ph), 7.52−7.56 (m, 2 H, *m*-Ph). − ^{13}C NMR ($CDCl_3$): δ = 20.5, 20.7 (s, 3 C, 3 CH_3CO), 55.6 (s, 1 C, OCH_3), 59.2, 61.4, 63.0, 67.0, 68.6, 69.1, 70.9, 71.1, 75.8, 75.9 (s, 10 C, C2, C3, C4, C5, C6, C2′, C3′, C4′, C5′, C6′), 99.6, 100.6, 102.4 (s, 3 C, PhCH, C1, C1′), 126.1, 128.1, 128.9 (s, 6 C, Ph), 170.2, 170.3 (s, 4 C, 4 CH_3CO). − $C_{28}H_{35}N_3O_{14}$ (637.6): calcd. C 52.7, H 5.53; found C 52.3, H 5.63.

Methyl *O*-(2,3,4,6-Tetra-*O*-acetyl-β-D-galactopyranosyl)-(1→3)-4,6-di-*O*-acetyl-2-azido-2-deoxy-α-D-galactopyranoside (11): A solution of **10** (275 mg, 0.431 mmol) was stirred overnight with a mixture of acetic acid and water (80:20 v/v) at 45 °C, evaporated in vacuo, and co-distilled four times with toluene. The residual colorless foam was stirred overnight with acetic anhydride and pyridine, evaporated in vacuo, and co-distilled with toluene. The residue was chromatographed on silica gel (*l:* 23 cm, *d:* 2 cm, ea/hx 3:2), evaporated in vacuo, and co-distilled with toluene and dichloromethane. A colorless solid was isolated (230.9 mg, 84.5%); m.p. 157−159 °C; $[\alpha]_D^{23}$ = +95.4 (*c* = 0.86, $CHCl_3$); R_f = 0.55 in ea/hx 2:1. − ^{1}H NMR ($CDCl_3$): δ = 1.98, 2.05, 2.06, 2.07, 2.13, 2.16 (s, 18 H, 6 CH_3CO), 3.43 (s, 3 H, OCH_3), 3.72 (dd, 1 H, $J_{1,2}$ = 3.57, $J_{2,3}$ = 10.70 Hz, H2), 3.89 (dt, 1 H, $J_{4',5'}$ = 0.82 Hz, $J_{5',6a'}$ = 6.72 Hz, $J_{5',6b'}$ = 7.00 Hz, H5′), 4.00 (dd, 1 H, $J_{6a',6b'}$ = 11.25 Hz, H6b′), 4.09 (dd, 1 H, $J_{3,4}$ = 3.29 Hz, H3), 4.06−4.12 (m, 2 H, H5, H6b), 4.15 (dd, 1 H, H6a′), 4.16 (dd, 1 H, $J_{5,6a}$ 4.12 Hz, $J_{6a,6b}$ = 11.39 Hz, H6a), 4.70 (d, 1 H, $J_{1',2'}$ = 7.82 Hz, H1′), 4.87 (d, 1 H, H1), 5.00 (dd, 1 H, $J_{2',3'}$ = 10.43 Hz, $J_{3',4'}$ = 3.43 Hz, H3′), 5.17 (dd, 1 H, H2′), 5.36 (dd, 1 H, H4′), 5.45 (dd, 1 H, $J_{4,5}$ = 0.41 Hz, H4). − ^{13}C NMR ($CDCl_3$): δ = 20.5, 20.6, 20.7 (s, 6 C, 6 CH_3CO), 55.4 (s, 1 C, OCH_3), 59.8, 61.0, 62.7, 66.8, 69.5, 70.8, 74.7, 70.8 (s, 10 C, C2, C3, C4, C5, C6, C2′, C3′, C4′, C5′, C6′), 98.7, 101.5 (s, 2 C, C1, C1′), 169.5, 169.7, 170.1, 170.3, 170.4, 170.5 (s, 6 C, 6 CH_3CO). − $C_{25}H_{35}N_3O_{16}$ (633.6): calcd. C 47.4, H 5.57; found C 47.8, H 5.75.

Methyl *O*-(2,3,4,6-Tetra-*O*-acetyl-β-D-galactopyranosyl)-(1→3)-2-acetamido-4,6-di-*O*-acetyl-2-deoxy-α-D-galactopyranoside (12): Disaccharide **11** (220.0 mg, 0.347 mmol) was stirred overnight, under an N_2 atmosphere, with thioacetic acid (0.75 mL, 10.49 mmol), evaporated in vacuo, and co-distilled several times with toluene. The residual oil was chromatographed on silica gel (*l:* 26 cm, *d:* 2 cm, first 100 mL ea/hx 5:1, then ea). After evaporation and azeotropic distillation with toluene and dichloromethane, a colorless foam was isolated (141.8 mg, 62.9%); R_f = 0.25 in ea/hx 15:1. − ^{1}H NMR ($CDCl_3$): δ = 2.01 (s, 3 H, $NHCOCH_3$), 1.97, 2.06, 2.08, 2.14, 2.17 (s, 18 H, 6 CH_3CO), 3.38 (s, 3 H, OCH_3), 3.87 (dt, 1 H, $J_{5',6a'/b'}$ = 6.91 Hz, H5′), 3.92 (dd, 1 H, $J_{2,3}$ = 11.06, $J_{3,4}$ = 3.32 Hz, H3), 3.98−4.22 (m, 6 H, H4, H5, H6a, H6b, H6a′, H6b′), 4.52 (ddd, 1 H, $J_{1,2}$ = 3.59 Hz, H2), 4.59 (d, 1 H, $J_{1',2'}$ = 8.02 Hz, H1′), 4.80 (d, 1 H, H1), 4.95 (dd, 1 H, $J_{2',3'}$ = 10.50 Hz, $J_{3',4'}$ = 3.46 Hz, H3′), 5.13 (dd, 1 H, H2′), 5.36 (dd, 1 H, $J_{4',5'}$ = 0.97 Hz, H4′), 5.63 (d, 1 H, $J_{2,NH}$ = 8.98 Hz, NH). − ^{13}C NMR ($CDCl_3$): δ = 20.4−20.8 (m, 6 C, 6 CH_3CO), 23.3 (s, 1 C, $NHCOCH_3$), 55.3 (s, 1 C, OCH_3), 48.8, 61.0, 62.7, 66.7, 67.2, 68.4, 68.9, 70.7, 72.8, 77.4 (s, 10 C, C2, C3, C4, C5, C6, C2′, C3′, C4′, C5′, C6′), 98.6, 100.6 (s, 2 C, C1, C1′), 169.7, 170.1, 170.3, 170.4, 170.5 (s, 7 C, 7 CH_3CO).

Methyl *O*-(β-D-Galactopyranosyl)-(1→3)-2-acetamido-2-deoxy-α-D-galactopyranoside (13): A solution of **12** (107.0 mg, 0.165 mmol) in dry methanol (25 mL) was mixed with a fresh solution of sodium in dry methanol (50 µL, 9.43 µmol) and stirred for 90 min, neutralized with Amberlite® IR-120, filtered, evaporated in vacuo, and co-distilled with toluene and dichloromethane. The residual colorless solid was chromatographed on silica gel (*l:* 17 cm, *d:* 2 cm, first ea, then MeOH/$CHCl_3$ 4:5). After evaporation and azeotropic distillation with toluene and dichloromethane, a colorless solid was isolated (58.8 mg (89.7%); m.p. >235 °C (decomp.); $[\alpha]_D^{23}$ = +127.9 (*c* = 0.38, water); R_f = 0.20 in $CHCl_3$:MeOH 5:4. − ^{1}H NMR (TSP): δ = 2.03 (s, 3 H, $NHCOCH_3$), 3.40 (s, 3 H, OCH_3), 3.53 (dd, 1 H, $J_{1',2'}$ = 7.78 Hz, $J_{2',3'}$ = 9.92 Hz, H2′), 3.62 (dd, 1 H, $J_{3',4'}$ = 3.36 Hz, H3′), 3.66 (dd, $J_{5',6a'}$ = 7.96 Hz, $J_{5',6b'}$ 9.88 Hz, H5′), 3.71−3.81 (m, 4 H, H6a, H6b, H6a′, H6b′), 3.92 (d, 1 H, H4′), 3.95 (t, 1 H, $J_{5,6ab}$ = 5.95 Hz, H5), 4.00 (dd, 1 H, $J_{2,3}$ = 10.99, $J_{3,4}$ = 3.05 Hz, H3), 4.23 (d, 1 H, $J_{4,5}$ = 2.59 Hz, H4), 4.34 (dd, 1 H, $J_{1,2}$ = 3.66 Hz, H2), 4.47 (d, 1 H, H1′), 4.79 (d, 1 H, H1). − ^{13}C NMR (TSP): 22.2 (s, 1 C, $NHCOCH_3$), 48.7 (s, 1 C, C2), 55.3 (s, 1 C, OCH_3), 61.1, 61.3 (s, 2 C, C6, C6′), 68.7 (s, 1 C, C4′), 68.8 (s, 1 C, C4), 70.5 (s, 1 C, C5), 70.8 (s, 1 C, C2′), 72.7 (s, 1 C, C3′), 75.1 (s, 1 C, C5′), 77.4 (s, 1 C, C3), 98.4 (s, 1 C, C1), 104.7 (s, 1 C, C1′), 174.7 (s, 1 C, $NHCOCH_3$).

Acknowledgments

This work was supported by grants from the Deutsche Forschungsgemeinschaft (to T.W.), the federal state of Schleswig-Holstein (to R.B.), NATO (CRG # 961220) and the NIH (to R.W. NIGMS-55230). We want to thank Prof. Hans Paulsen, Hamburg, for stimulating discussions about the synthesis of the disaccharide and a gift of some starting material. Dr. Englbert Bäuml provided helpful references for modern synthetic methodologies, and Prof. Thomas Peters is thanked for giving us access to the NMR and computing facilities in Lübeck.

[1] M. Verma, E. A. Davidson, *Glycoconjugate J.* **1994**, *11*, 172−179.
[2] R. E. Feeney, Y. Yeh, *Adv. Protein Chem.* **1978**, *32*, 191−282.
[3] G. F. Springer, *Crit. Rev. Oncogen.* **1995**, *6*, 57−85.
[4] F.-G. Hanisch, S. E. Baldus, *Histol. Histopatol.* **1997**, *12*, 263−281.
[5] S. W. Homans, A. L. DeVries, S. B. Parker, *FEBS Lett.* **1985**, *183*, 133−136.
[6] C. A. Bush, R. E. Feeney, *Int. J. Peptide Protein Res.* **1986**, *28*, 386−397.
[7] P.-E. Jansson, G. Widmalm, *J. Chem. Soc., Perkin Trans. 2* **1992**, 1085−1090.
[8] A. Pollex-Krüger, B. Meyer, R. Stuike-Prill, V. Sinnwell, K. L. Matta, I. Brockhausen, *Glycoconjugate J.* **1993**, *10*, 365−380.
[9] S. Hanessian, H. Hori, Y. Tu, Y. Boullanger, *Tetrahedron* **1994**, *50*, 77−92.
[10] A. Imberty, E. Mikros, J. Koča, R. Mollicone, R. Oriol, S. Pérez, *Glycoconjugate J.* **1995**, *12*, 331−349.
[11] H. Paulsen, J.-P. Hölck, *Carbohydr. Res.* **1982**, *109*, 89−107.
[12] H. Paulsen, M. Paal, M. Schultz, *Tetrahedron Lett.* **1983**, *24*, 1759−1762.
[13] H. Paulsen, M. Paal, *Carbohydr. Res.* **1984**, *135*, 53−69.

[14] H. Paulsen, M. Paal, *Carbohydr. Res.* **1984**, *135*, 71−84.
[15] M. Mikamo, *Carbohydr. Res.* **1989**, *191*, 150−153.
[16] R. R. Schmidt, J. Michel, M. Roos, *Liebigs Ann. Chem.* **1984**, 1343−1357.
[17] G. Grundler, R. R. Schmidt, *Liebigs Ann. Chem.* **1984**, 1826−1847.
[18] R. U. Lemieux, R. M. Ratcliffe, *Can. J. Chem.* **1979**, *57*, 1244−1251.
[19] N. Ikemoto, O. K. Kim, L.-C. Lo, V. Satyanarayana, M. Chang, K. Nakanishi, *Tetrahedron Lett.* **1992**, *33*, 4295−4298.
[20] T. Weimar, R. Bukowski, N. M. Young, *J. Biol. Chem.* **2000**, *275*, 37006−37010.
[21] T. Peters, T. Weimar, *J. Biomol. NMR* **1994**, *4*, 97−116.
[22] C. Landersjö, R. Stenutz, G. Widmalm, *J. Am. Chem. Soc.* **1997**, *119*, 8695−8698.
[23] J.-F. Espinosa, F. J. Cañada, J. L. Asensio, M. Martín-Pastor, H. Dietrich, M. Martín-Lomas, R. R. Schmidt, J. Jiménez-Barbero, *J. Am. Chem. Soc.* **1996**, *118*, 10862−10871.
[24] J. F. Espinosa, E. Montero, A. Vian, J. L. García, H. Dietrich, R. R. Schmidt, M. Martín-Lomas, A. Imberty, F. J. Cañada, J. Jiménez-Barbero, *J. Am. Chem. Soc.* **1998**, *120*, 1309−1318.
[25] X. Lee, A. Thompson, Z. Zhiming, H. Ton-that, J. Biesterfeldt, C. Ogata, L. Xu, R. A. Z. Johnston, N. M. Young, *J. Biol. Chem.* **1998**, *273*, 6312−6318.
[26] R. Stuike-Prill, B. Meyer, *Eur. J. Biochem.* **1990**, *194*, 903−919.
[27] R. Boelens, T. M. G. Koning, G. A. Van der Marel, J. H. Van Boom, R. J. Kaptein, *J. Magn. Reson.* **1989**, *82*, 290−308.
[28] B. A. Borgias, T. L. James, *Methods Enzymol.* **1989**, *176*, 169−183.
[29] R. J. Woods, R. A. Dwek, C. J. Edge, B. Fraser-Reid, *J. Phys. Chem.* **1995**, *99*, 3832−3846.
[30] D. A. Case et al., *AMBER 5.0.* **1997**, University of California, San Francisco, USA.
[31] T. James, H. E. Leu, *CORMA*, **1999**, University of California, San Francisco, USA.
[32] P. J. Kraulis, *J. Appl. Crystallogr.* **1991**, *24*, 946−950.
[33] L.-F. Tietze, T. Eicher, *Reaktionen und Synthesen im organisch-chemischen Praktikum*, Thieme-Verlag, Stuttgart, **1981**, 482 ff.
[34] J. Broddefalk, U. Nilsson, J. Kihlberg, *J. Carbohydr. Chem.* **1994**, *13*, 129−132.
[35] L. Somsák, I. Németh, *J. Carbohydr. Chem.* **1993**, *12*, 679−684.
[36] P. J. Garegg, C.-G. Swahn, *Meth. in Carbohydr. Chem.* **1980**, Vol. VII, Academic Press, London, 317−319.

Received October 19, 2000
[O00531]